Investigating the Dosimetry Potential of the NIPAM Polymer Gel

by

Chibuike D. Umeh

Duke Kunshan and Duke University

Medical Physics Program

Date: _____

Approved:

_____

Justus Adamson, Supervisor

_____

Mark Oldham

_____

William Giles

_____

David Huang

Thesis submitted in partial fulfillment of
the requirements for the degree of Master of Science, in
Duke Kunshan and Duke University
Medical Physics Program in the Graduate School
of Duke University

2019

ABSTRACT

Investigating the CT Dosimetry Potential of the NIPAM Polymer Gel

by

Chibuike D. Umeh

Duke Kunshan and Duke University

Medical Physics Program

Date: _____

Approved:

_____

Justus Adamson, Supervisor

_____

Mark Oldham

_____

William Giles

_____

David Huang

An abstract of a thesis submitted in partial
fulfillment of the requirements for the degree
of Master of Science, in
Duke Kunshan and Duke University
Medical Physics Program in the Graduate School of
Duke University

2019

Abstract

Purpose: The aim of this work is to assess the potential of applying NIPAM polymer gel produced at Duke for CT and CBCT on board imaging for radiation therapy. This is after initial progress has been made in establishing the potential of using this gel but produced at a different location to visualize the dose for multitarget radiosurgery using the KV-CBCT system mounted on-board the linear accelerator.

Materials and Methods: A reproducible procedure for manufacturing polymer gel developed by previous researchers in this field was implemented at the 3D Dosimetry and Bio – imaging lab at Duke University. The use of vacuum seal and oil was introduced as an additional means of minimizing oxygen contamination immediately after production. The technique is to apply the gel for CBCT and sheet Dosimetry CBCT-Dosimetry: The CBCT acquisition and reconstruction parameters were optimized to maximize low contrast resolution. Varian 600C/D linear accelerator whose QA test has been successful and already in clinical use for SRS was used for spot check. Six different angles were made for each of the gantry, collimator and couch rotations. The radiation isocenter was quantified by determining the center of the smallest intersecting circle; the 3D vector coincidence with the imaging coordinate system was also quantified.

Sheet Dosimetry: A Flat shaped gel was prepared in a vacuum sealed bag. Ten different MU values were delivered at different spots of the gel using the Varian 600C/D linear accelerator which was later scanned using the EPSON flatbed scanner and Diagnostic CT. The optical density values were determined in the three color bands; likewise variation of the mean CT number with dose.

Results: CBCT-D: The optimal values for our CBCT setting were full trajectory, smooth reconstruction filter, strong ring suppression and 80KV. For the star shots, the radius of the smallest circle was 0.5mm, 0.3mm, and 0.6mm for the gantry, couch, and collimator, which were within the recommended tolerance limits specified by TG142 and were within 0.2mm of the value obtained from a traditional film star shot. The 2D vector discrepancy from the imaging coordinate system was 0.1mm, 1.3mm and 1.5mm for the gantry, couch, and collimator, respectively.

Sheet: The optical density values increased with increasing MU in the three color channels. The blue channel showed the largest change in optical density (24% difference); while the red color showed the least. The diagnostic scan showed a linear increase of CT number with MU. At lower MU (0 – 200), the increase fluctuated due to background noise and dose scatter. Above 200MU showed a linear increase in polymerization.

Conclusion: All the irradiated spots and spoke polymerized to the degree of radiation dose quantity and easily visible; which supports the feasibility of the NIPAM polymer gel produced at Duke for dose distribution and QA test. Specifically, the calibration potential of the polymer gel when used as sheet for both the optical and diagnostic CT scan has now been established.

Dedication

This work is dedicated to all scholars who against all odds strive to contribute in any way to the fight against cancer in the sub-Sahara African region

Contents

List of Tables

List of Figures

Acknowledgements

Justus Adamson, PhD

William Giles, PhD

Mark Oldham, PhD

Paul Yoon, PhD

James Bowsher, PhD

David Huang, PhD

Claire Kaimei Luo

Class of 2019 Duke & DKU students

Ogenna Umeh

1. Introduction

In the past two decades, new technologies have been added to the medical linear accelerator leading to new treatment techniques in clinical practice such as asymmetrical jaws, dynamic and virtual wedges, multi leaf collimators (MLC), intensity modulated radiotherapy (IMRT), stereotactic radiosurgery (SRS), and Stereotactic Body Radiation Therapy (SBRT). These innovations enable steep dose gradient between the treatment volume and normal tissues but have yet to be matched with corresponding dose measurement techniques. The gap now is to find a dosimetry technique that allows full 3D dose measurement with high precision and optimum spatial resolution and integrity.

The most common technique for 2D dosimetry measurements is radiochromic film, which can provide radiation treatment dose verification and measure 2D dose maps in external beam radiation therapy (EBRT) with high resolution (Tamponi, Bona, Poggiu, & Marini, 2015). Although a semi-complete three-dimensional (3D) dose measurement could be produced by positioning film in multiple planes, accurate positioning can be difficult and time-consuming. Specialized detector arrays are often used to verify dose distributions; one example is the Delta4 device (ScandiDos, Uppsala, Sweden) which is a 3D diode array consisting of diode matrices in two orthogonal planes inserted in a cylindrical acrylic phantom which is a complex device for IMRT

verification (Bedford, Lee, Wai, South, & Warrington, 2009; Petoukhova, van Egmond, Eenink, Wiggenraad, & van Santvoort, 2011). A second example is ArcCHECK, a cylindrical diode array. These devices are more convenient but can only provide a limited sample of the dose distribution.

Polymer gel dosimeters are potentially an ideal dosimeter (Alber et al., 2008) that integrates the time-dependent 3D spatial distribution of dose delivery during IMRT. Polymer gel dosimetry has historically been limited by the toxicity of ingredients and potential oxygen contamination of the dosimeter. The ideal dosimeter for clinical use should be a normoxic gel with no toxicity. The Polyacrylamide gel dosimeter (PAG) which has been in use is toxic and hypoxic or anoxic. The MAGIC polymer gel formulation or nPAG consisted of Methacrylic acid, Ascorbic acid, Gelatin and Copper developed by Fong, Keil, Does, & Gore (2001) replaced the PAG because it is a normoxic gel. The ascorbic acid binds free oxygen contained within the aqueous gelatin matrix into metallo-organic complexes in a process initiated by copper sulfate (Baldock et al., 2010; Deene, Venning, Hurley, Healy, & Baldock, 2002). Senden, Jean, McAuley, & Schreiner (2006) introduced and investigated the dose response of three new reduced toxic gel dosimeters. One of which is the N-isopropylacrylamide (NIPAM) polymer gel. In this gel, the more toxic acrylamide in the nPAG was replaced with the less harmful

monomers N-isopropylacrylamide (NIPAM). Jirasek et al., (2015) and F Pak et al., (2012) assessed the dosimetric properties of NIPAM polymer gel dosimeter: reproducibility, linearity, tissue equivalency, dose rate and energy independency; and found out that it is very promising in all aspects of the assessed properties.

Many gel dosimeters are water-equivalent and can itself constitute the anthropomorphic phantom, making it free from dose perturbation effects. Polymer gel dosimeters have been applied for measuring 3-dimesional radiation dose distributions in radiotherapy (Farideh Pak, Farajollahi, Movafaghi, & Naseri, 2013). Polymer gel offers a method of acquiring 3D maps of complex radiotherapy dose distributions with a spatial resolution of the order of 1 mm, depending upon the scanning and imaging specifications (Mcjury et al., 2000). The gel dosimeters are made from radiation sensitive chemicals which are radiologically equivalent to soft tissue. When it interacts with radiation, radiolysis occurs. The water molecules are dissociated into several highly reactive radicals and ions. The radicals initiate the polymerization of monomers by reacting with the monomers in chains (Baldock et al., 2010). The amount of polymerization is a function of the absorbed radiation dose. It records radiation dose distribution in three-dimensions (3D), and is well suited where steep dose gradients exist such as in intensity-modulated radiation therapy (IMRT) and SRS (Baldock et al.,

2010). The chemical changes caused by the dose can be read out using a number of technologies including MRI(De Deene et al., 1998; Gustavsson et al., 2003), optical CT (Oldham et al., 2001), ultrasound (Mather, Whittaker, & Baldock, 2002), as well as x-ray CT (Hilts, Audet, Duzenli, & Jirasek, 2000).

Dose readout by X-ray CT has a few advantages including the widespread availability of CT scanners, and the well quantified spatial integrity of the resulting CT images. Advances in this technique have included developing a more sensitive dosimeter (Jirasek, Hilts, & McAuley, 2010; Jirasek et al., 2015), identifying optimal CT acquisition parameters (Hilts, Jirasek, & Duzenli, 2005), and application to multislice CT (Johnston, Hilts, & Jirasek, 2015). X-ray CT is based on radiation induced polymerization causing a change in the absorption coefficient of the irradiated polymer gel (Baldock et al., 2010). This change in linear attenuation coefficient is mainly attributed to a change in electron density originating from the expulsion of water in the polymer clusters which is then related to an associated change in mass density (Brindha, Venning, Hill, & Baldock, 2004; Trapp, Michael, Deene, & Baldock, 2002). The relative mass density change is in the order of 1 mg cm−3 Gy−1 (Trapp, Bäck, Lepage, Michael, & Baldock, 2001) and results in a change in CT number in the order of 1 Hounsfield unit per Gray. The limitation of this technology is low sensitivity. The low CT dose

sensitivity of polymer gel dosimeters implies that, several imaging averages have to be taken for each slice in order to use x-ray CT for radiation dosimetry purposes (Baldock et al., 2010). The Signal to Noise Ratio (SNR) is proportional to the square root of N, where N is the number of averages. It has been shown that typically between 16 and 32 image averages provide a reasonable trade-off between SNR improvement and imaging time and tube load (Hilts et al., 2005).

Most recently, the kV-CBCT system mounted on-board a linear accelerator was utilized to visualize the dose for multitarget radiosurgery delivered to a NIPAM dosimeter (Adamson et al., 2018). Image Guided Radiotherapy (IGRT) is a commonly applied clinical technique in which an imaging system that is integrated with the clinical linear accelerator such as kV-CBCT is utilized to align the patient prior to delivering the radiotherapy treatment. This serves to improve the precision and accuracy of the delivery of radiation treatment. Using on-board kV-CBCT to image the dose from a polymer gel dosimeter has the added advantage that the dose is read out using the same imaging / coordinate system that is used to set up patients, thus uniquely quantifying spatial agreement between the imaging and radiation systems. This recent work represented a first step towards utilizing CBCT for polymer gel dosimetry; here we

build upon this work by further optimizing the technique and developing further applications.

The general objective of this study is to apply NIPAM 3D dosimetry to CT & CBCT imaging. Specifically, in Chapter 2 we describe utilization of the kV-CBCT system mounted on-board a linear accelerator to quantify dose to a traditional cylindrical 3D dosimeter. We determine the optimal CBCT acquisition settings, and then apply this technique for a practical clinical application (quantifying radiation isocenter wobble, or "star shot"). Then, in Chapter 3, we describe development of unique flat NIPAM 3D dosimeters with film characteristics, as well as the demonstrating the feasibility of utilizing a dual dose calibration (density from CBCT and optical density from a flat-bed scanner

2. Cone beam CT Dosimetry (CBCT –D)

The overall goal of this chapter is to apply CBCT for dose readout of x–ray CT polymer gel dosimetry. To accomplish this, we developed a CBCT dosimetry program which will be reproducible here at Duke for clinical tasks. Recently, our research group demonstrated the feasibility of utilizing the kV-CBCT system mounted on-board a linear accelerator to readout the dose distribution for multi-target radiosurgery (Adamson et al., 2018). They showed for the first time that dose from NIPAM dosimeters could be visualized using KV-CBCT and this dose could be extracted immediately after irradiation. It also demonstrated that the dosimeter could be manufactured in one location and irradiated in a second (remote) location. However, the CBCT technique was selected with little thought of optimizing the imaging parameters. Now, we decided to improve on this work by producing the dosimeter here in Duke thereby eliminating the logistics of transportation with controlled temperature and create a feasibility for in depth analysis. Secondly, optimize the CBCT acquisition technique for better image quality of the gel.

2.1 Materials and Methods

2.1.1 Dosimeter preparation

The first aim was to develop a procedure for manufacturing NIPAM dosimeters at the 3D Dosimetry and Optical Bio-Imaging Lab at Duke University. The laboratory

method was adopted on the procedures of (Jirasek et al., 2012; Maynard, Hilts, Heath, & Jirasek, 2017; Senden et al., 2006). This process creates room for flexibility and reproducibility in the making process.

All gel materials consisted of, by weight (*1g =1ml for pure water of density 1g/ml*)

- 75.5% deionized water
- 5% gelatin (Sigma-Aldrich, Oakville, ON, Canada),
- 15% N-isopropylacrylamide (NIPAM)
- 4.5% N,N'-methylenebisacrylamide (BIS, Sigma-Aldrich) and
- 5 mM tetrakis hydroxymethyl phosphonium chloride (THPC, Sigma-Aldrich)

The formulation process has 4 steps: Each step of the procedure is carefully controlled based on timing and temperature, to ensure reproducibility (1): Gelatin (300 Bloom Type A) was allowed to swell in the 75.5% of the de-ionized water for 10 min at room temperature, before heating to 45 ◦C. (2): While stirring continuously, Bis was dissolved at 45 °C, which took about 15 min, followed by addition of monomer (NIPAM). The gelatin–crosslinker mixture had to cool to approximately 37 °C. (3): A solution of the antioxidant THPC was added to the solution. The resulting gels were clear (the Bis gel was very faint yellow) and transparent. (4): The gel solutions were transferred into a plastic container with low oxygen permeability, and then closed with a sealing film.

2.1.2 Optimizing the CBCT Acquisition & Reconstruction Parameters for CBCT-Dosimetry

In this section, our goal was to determine the best CBCT acquisition and reconstruction settings to maximize the sensitivity of the 3D dosimetry system. This is because the density change in the dosimeter is relatively little compared to the sensitivity of other measurements (MRI / optical density from optical CT) and CBCT is noisier than diagnostic CT. If a single CBCT is acquired, then the image noise is limited by the maximum available mAs. However, if multiple CBCTs are to be averaged, then the limiting factor will be the heat loading on the x-ray tube and waiting for the tube to cool. For this measurement, we utilized a Truebeam STX (Varian, Palo Alto CA) linear accelerator equipped with an on-board kV-CBCT system. The tradeoff between image quality and anode heating limit was investigated for our CBCT-Dosimetry using the CATPHAN® 500. The Catphan® 500 provides a comprehensive set of measurements to measure the maximum performance of the CT scanner's sensitometry, uniformity, geometric and low-contrast sensitivity ("Catphan 500 — The Phantom Laboratory," n.d.). Our work is to focus on the maximizing the low contrast resolution.

Table 1: Adjustable settings for improved image quality

Acquisition Parameters	**Settings**
Fan type	Full
Trajectory	Full vs Half
Kilovoltage	80, 100 & 125
mAs	400 – 7000
Reconstruction Parameters	
Reconstruction filter	Smooth, Standard, Sharp, Auto and Ultrasharp
Ring suppression	Disabled, WeaK, Medium and Strong
Matrix size	512
Slice thickness	2mm

Note: The Matrix size and Slice thickness is adjustable; but was kept constant for this study

The method was to first determine the mAs per kV that gives equal loading on the heat tube, and then determine for each kV the total Contrast as well as Contrast to Noise Ratio (CNR) but using the mAs that gives the same x-ray tube heat loading. We also investigated optimizing the reconstruction parameters to maintain high Contrast and CNR of the measured dose distribution. The reconstruction settings that were available to modify include filtration technique (Smooth, Standard, Sharp, Auto

and Ultrasharp) and ring suppression (Disabled, Weak, Medium and Strong). The full setting parameters could be viewed in Table 1

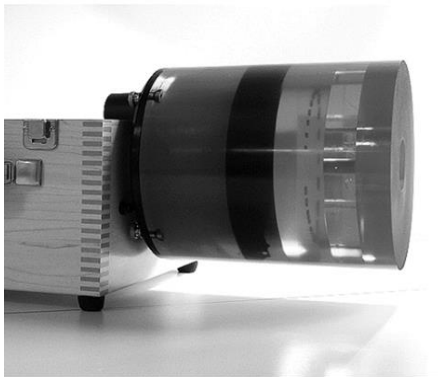

Figure 1: CAT phantom used for analysis of CBCT image quality ("Catphan 500 — The Phantom Laboratory," n.d.)

The Phantom scan

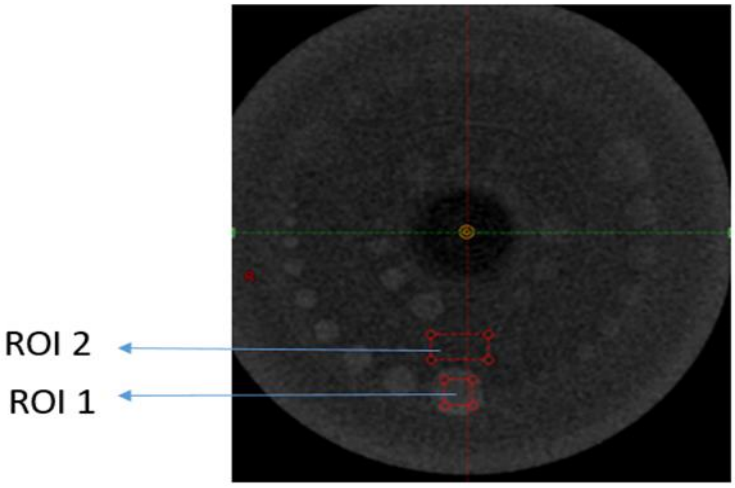

Figure 2: The axial section of the phantom scan

ROI 1: Region of Interest 1 ROI 2: Region of Interest 2

The red square within the circle is the image signal (1) used to determine the contrast; while the red rectangle is the background signal (2). The Contrast (C) and Contrast to Noise Ratio (CNR) are given as

C = Mean ROI 1 – Mean ROI 2

CNR = C/σ

Where σ is the standard deviation of the pixels within ROI 2

The ROI for image signal and background signal are defined as a shell describing a volume located 0.5 cm to 1.5cm around the selected image signal and selected background signal. The ROI image signal selection is done to exclude areas within 0.5cm of background signal, dosimeter edges or any close by signal affecting the defined volume; also similar to the ROI background signal selection which is based on avoiding image signal influence in the defined background signal.

2.1.3 Clinical application of CBCT –D for verification of radiation isocenter

Once the technique was developed for manufacturing dosimeters at the 3D Dosimetry and Optical Bio-Imaging Lab at Duke, and an acceptable CBCT acquisition and reconstruction technique was identified, we demonstrated the functionality of the dosimetry system by applying a practical clinical application. An ideal isocenter is the point at which the axes of rotation of the gantry, collimator and couch intersect. In reality, some uncertainty exists in the stability of the isocenter over the range of motion. A star shot is a test used in determining the location and uncertainty of the isocenter.

Conventionally, star shot is carried out using radiographic film. It captures the trajectory of a narrow radiation field at varying angles. Then the central rays of the beams are delineated and analyzed to verify that their intersections are contained within the tolerance range using a flatbed scanner. In place of a 3D dosimeter, the orientation of the films make up for this. González et al., (2004) used a five film orientation to determine the isocenter position and its size. Each film was placed in a plane perpendicular or parallel to one of the rotation axes in order to study the isocenter wobble in that particular plane or axial direction. The first film was placed in a plane perpendicular to the gantry axis and was irradiated at gantry angles of 0, 90, 225 and 315°. The second film was placed horizontally on the table and irradiated at gantry incidences of 0 and 180°. The third film was placed on the table horizontally and irradiated at couch angles of 0, 45, 90 and 315°. The fourth film was positioned vertically and the lasers were marked. The fifth film was used to determine the isocenter wobble due to collimator rotation; and it was placed horizontally on the table in a plane perpendicular to the collimator rotation axis. This procedure is sufficiently accurate, but can be time consuming due to the orientation arrangement and somewhat labor intensive due to the need to digitize the film for analysis.

In our own case, we used a 3D dosimeter and read it out using the CBCT. The star shot in the polymer gel is determined by placing the gel in the rotation plane of the motion under investigation. Then it is exposed to a collimated (small field size) radiation

beams from different angles of rotation such that the beams cross each other centrally in the gel. The crossing of the different fields forms a star-shaped pattern on the gel. A way of interpreting a star shot polymer gel is to assess visually the multi-axial symmetry of this star pattern. This symmetry is directly related to mechanical stability of rotation when the star shot fields are evenly spread over the range of rotation angles (Depuydt et al., 2012). Using the 3D dosimeter approach has two major advantages over the traditional film approach: (1) it automatically incorporates radiation vs imaging isocenter into the measurement, and (2) acquisition and analysis can utilize the kV-CBCT imaging system that is already incorporated into the radiation treatment device, as well as the treatment planning and record and verify systems rather than requiring a separate flatbed scanner as is the case for the traditional star shot.

For the star shot analysis, we measured the center of the smallest intersecting circle for all beams. This is a circle that forms tangent with the central line of all beams (coloured light green in Figure 3). The radius of this circle is called the radiation isocenter size – a quality measure for the rotational mechanical stability. Secondly, we also measured the discrepancy between the radiation isocenter and the imaging isocenter. Any deviation is represented by the three sides of the triangle (R, X, Y). Ideally, no deviation is expected; any non-zero value forms the accuracy of that dimension.

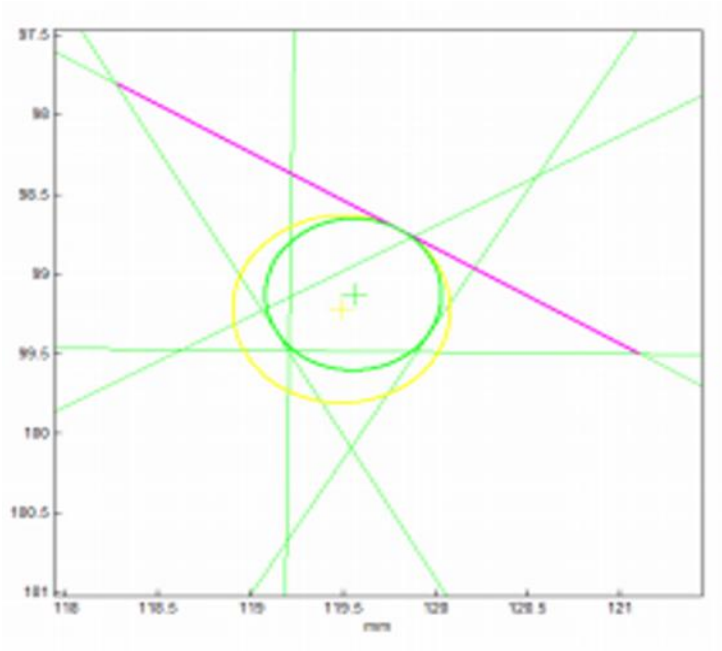

Figure 3: Traditional Winston Lutz analysis taken from the clinical annual QA report.

A secondary traditional analysis of the star shot is to compare the mechanical isocenter with the radiation isocenter using Figure 3. Each green line is the center of a beam profile. The light green cross at the center of the light green circle is the beam center. The purple line is the furthest distance between beam center intersections. The light green circle is the minimum tangent circle and the yellow circle is the maximum perpendicular distance to beam from the intersection center.

2.2 Results and Discussion

2.2.1 Dosimeter preparation

Figure 4: Making the dosimeter at Duke

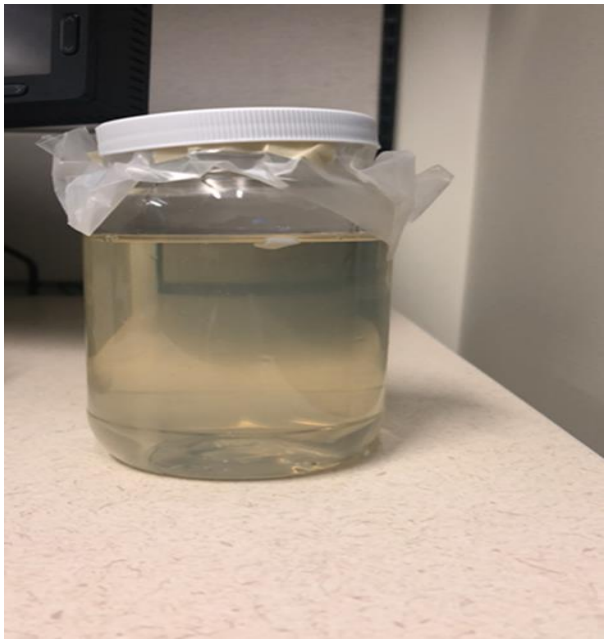

Figure 5: The completed NIPAM gel for CBCT-D

The total production time for the gel was approximately 1hour 20 minutes.

The first set of dosimeters we made had issues with low dose sensitivity at the periphery region due to oxygen contamination. A number of methods were tried to reduce this effect, including attaching oxygen absorbers at the lid of each container before sealing the dosimeter. However, this was not effective as it likely created non-perfect alignment of the lid to the container; thereby allowing oxygen to still get in; the oxygen absorbers also were problematic in that they caused artifacts in kV-CT and kV-CBCT images. In a second attempt, oil was poured at the gel surface after production to displace the air inside the container (above the gel). The dosimeter was then placed in a plastic bag used for food vacuum packaging, and a commercial vacuum packager (FoodSaver V3240) was used to remove the oxygen and seal the bag. This system removes air and moisture from specially designed, multi-layer bags while sealing.

2.2.2 CBCT acquisition technique

Table 2: Effect of mAs on contrast and CNR (Full scan vs Half scan)

This table shows the effect on image contrast and CNR for increasing mAs at 100KV, with all other parameters held constant. It is well known that as mAs increases, contrast remains constant while CNR improves, since noise decreases proportional to the mAs. As shown in the table, CNR increased as expected. The measure of contrast at the lowest mAs setting was subject to increased noise, leading to a more spurious measurement. Higher mAs values were used in subsequent tests. Comparison of full

scan versus half scan was made for the highest mAs which shows that the half scan showed a sharp drop in CNR which is expected due to the number of projection images acquired being roughly half.

mAs	***Contrast***	***CNR***
2714	31	5.0
4756	26	5.3
5058 (full scan)	26	5.9
5058 (Half scan)	26	1.3

Table 3: Effect of Reconstruction filter on Contrast

This table shows the effect on image contrast and CNR for different reconstruction filter at 100KV and mAs = 5058, with all other parameters held constant.

Reconstruction filter	***Contrast***	***CNR***
Smooth	26.2	9.0
Standard	28.4	6.9
Sharp	28.0	4.3
Auto (same as standard)	25.9	6.5
Ultra sharp	29.2	3.1

Table 4: Effect of Ring suppression on contrast and CNR

This table shows the effect on image contrast and CNR for different reconstruction filters at 125KV and mAs = 3420 with all other parameters held constant.

Ring Suppression	***Contrast***	***CNR***
Disabled	31	7.51
Weak	32	8.03
Medium	31	8.52
Strong	31	9.02

Table 5: Effect of kV on Contrast and CNR for equal tube heat loading

This table shows the effect of KV (Reconstruction filter: smooth, Ring suppression: Strong) but with heat loading held constant (hence different mAs settings). CNR increased markedly with increasing KV, while raw contrast was slightly higher for lower KV which is expected.

KV	*mAs*	*Contrast*	*CNR*
80	6052	32.4	7.61
100	5085	29.3	7.73
125	3420	30.8	9.02

Note: mAs Values were chosen not to overload the anode

The optimal values we decided for our CBCT setting were full trajectory, smooth reconstruction filter, strong ring suppression and 80KV. At this point, there was an upgrade so that the Ring Suppression could no longer be modified easily, so it was kept constant at the clinical setting (Medium) for later CBCT acquisitions.

2.2.3 Star shots

Post production to irradiation time was 72 hours for the gantry star shot, 48 hours for the collimator, and 24 hours for the couch. These different times was purely based on the availability of the linear accelerator. A total of 2000 Monitor Units (MU) were delivered per spoke based on our prior experience which showed adequate

contrast at dose levels above 10Gy. It was delivered at angles of 300, 330, 0, 30, 60 and 90 degrees for each of the rotations. All the gels polymerized in response to radiations.

2.2.3.1 Couch rotation (Oxygen and non-oxygen contamination effect)

Dose delivery at couch rotations were made to test for isocentric coincidence. Any mechanical misalignment will be displayed in the gel readily following this rotation. This creates a potential for the polymer gel dosimeter to be used for a quick quality assurance test prior to SRS session involving couch movements. The first dosimeter did not polymerize at the surface due to oxygen contamination (Figure 6). As a result of this, there is uncertainty in tracing the coincidence lines from the affected segment at the eclipse after the CBCT scan. To have confidence in the end result, we repeated the experiment; this time making a gel with special procedure to remove this oxygen contamination. The second gel polymerized all the way to the surface which was then used for other rotations and their CBCT scans

Figure 6: Star shot for Couch rotation (Oxygen and non-oxygen contamination effect)

2.2.3.2 Collimator rotation

We also tested isocentric coincidence for collimator rotation. Similar to couch rotations, changes in mechanical misalignment is displayed readily in the gel. The irradiated dosimeter is shown in Figure 7.

Figure 7: Star show for collimator rotation

2.2.3.3 Gantry rotation

This is similar to the couch and collimator rotation procedures mentioned earlier; but this time requiring gantry rotation. The irradiated dosimeter is shown in Figure 8

Figure 8: Star shot for gantry rotation

2.2.4 Pre and Post irradiation scanning

This scan is done using the CBCT optimized setting in Table 5 before and after the gel irradiation. The gel is immobilized with tape to the couch to prevent motion during the QA procedure.

Figure 9: CBCT-D set up of the gel for all-star shots

2.2.5 CBCT of star shots

2.2.5.1 Gantry rotation star shot

The CBCT of the irradiated dosimeter was analyzed by defining the center of the beam profile as a line between opposing ends and passing through the isocenter in the central axis CBCT image, as shown in Figure 10,Figure 11, Figure 12, Figure 13, Figure 14, Figure 15, and Figure 16 **.** A second magnified image centered on the isocenter region is also shown to visualize any misalignments.

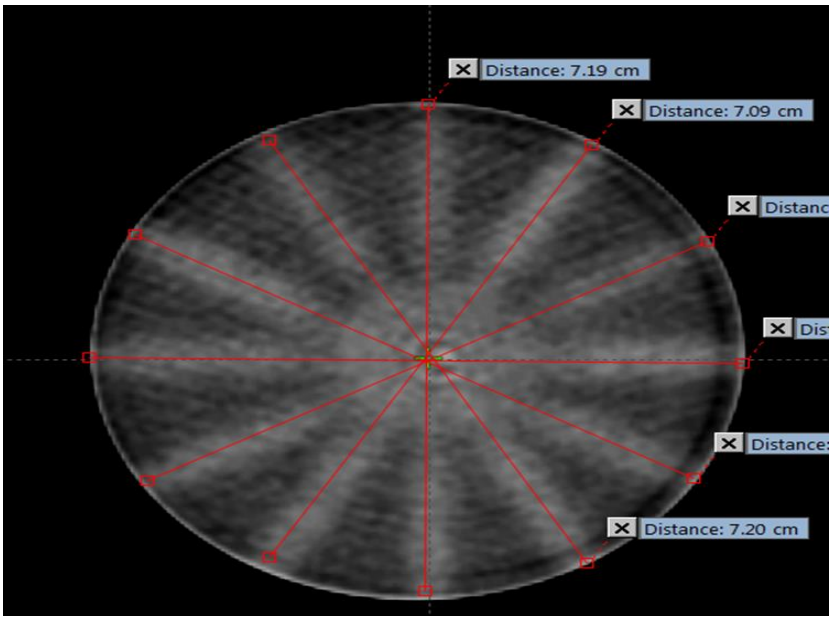

Figure 10: Gantry rotation star shot (Full circular scan)

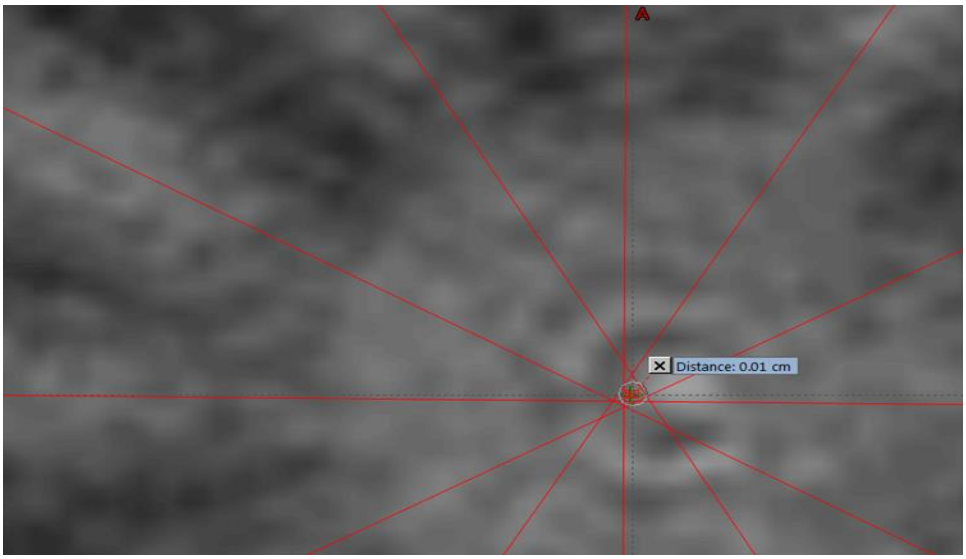

Figure 11: Gantry rotation star shot. (Zoomed isocentric region scan)

2.2.5.2 Couch rotation

This is similar to the explanation for the gantry rotation which is applied to the couch rotation.

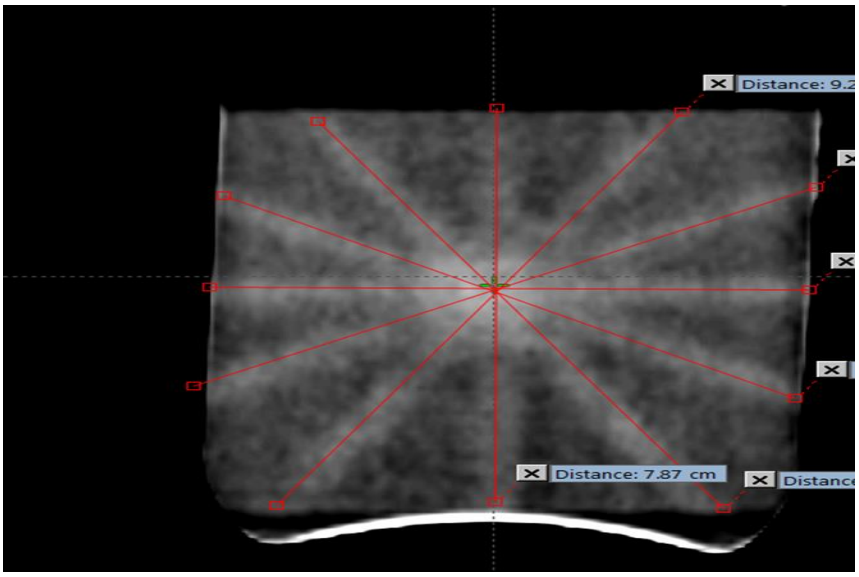

Figure 12: Couch rotation star shot. (Full circular scan)

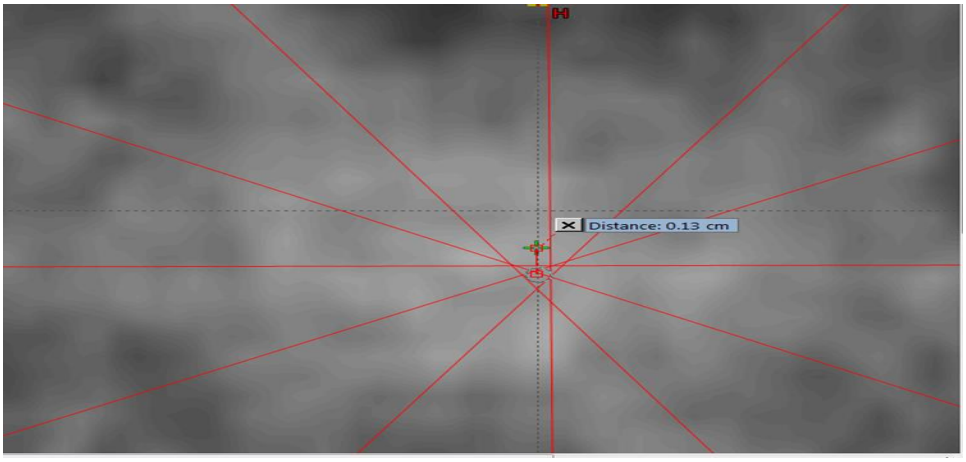

Figure 13: Couch rotation star shot. (Zoomed isocentric region scan)

2.2.5.3 Collimator rotation

2.2.5.3 Collimator rotation

This is similar to the explanation for the gantry rotation which is applied to the collimator rotation.

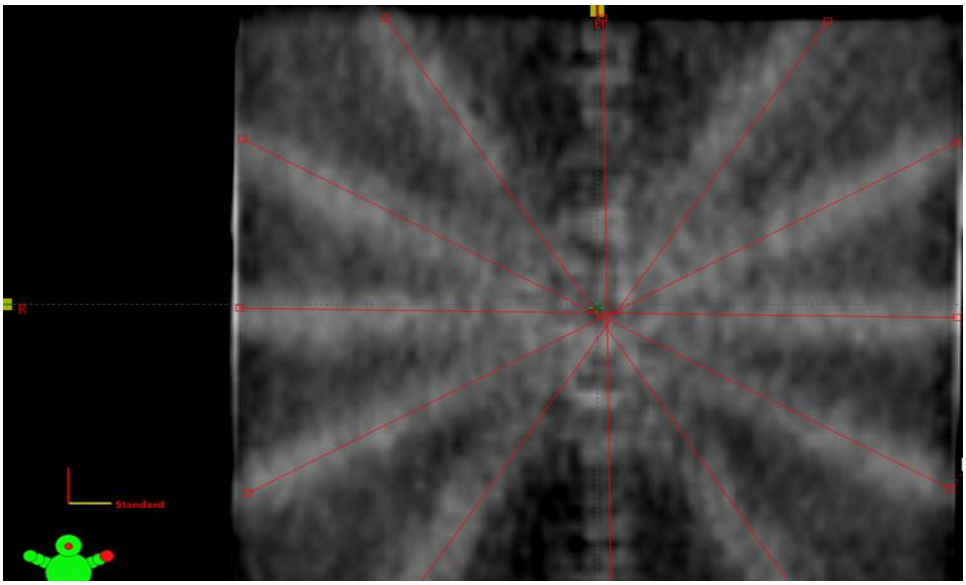

Figure 14: Collimator rotation star shot. (Full circular scan)

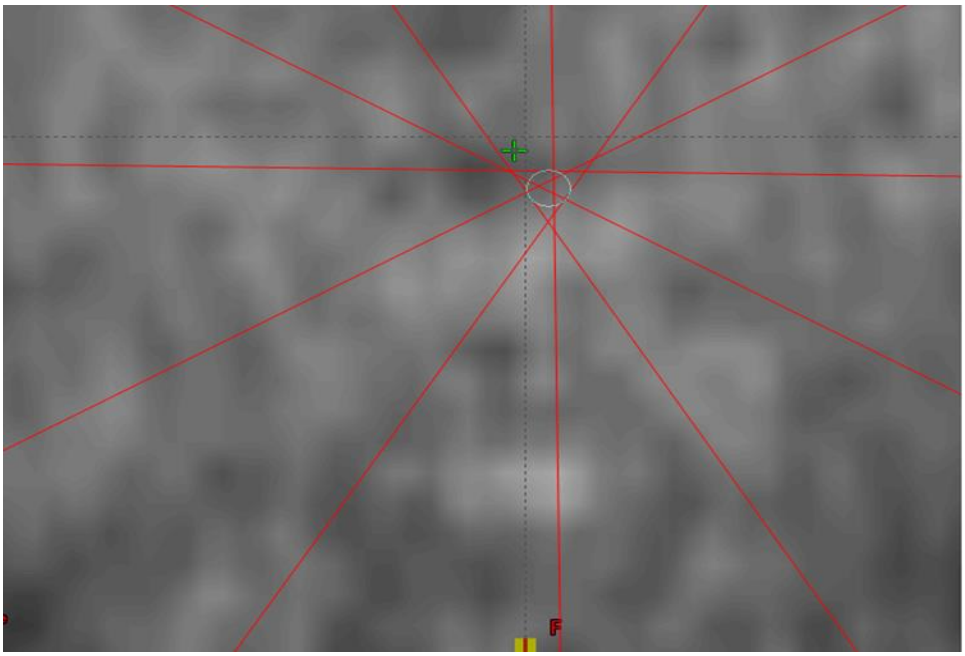

Figure 15: Collimator rotation star shot. (Zoomed isocentric region scan)

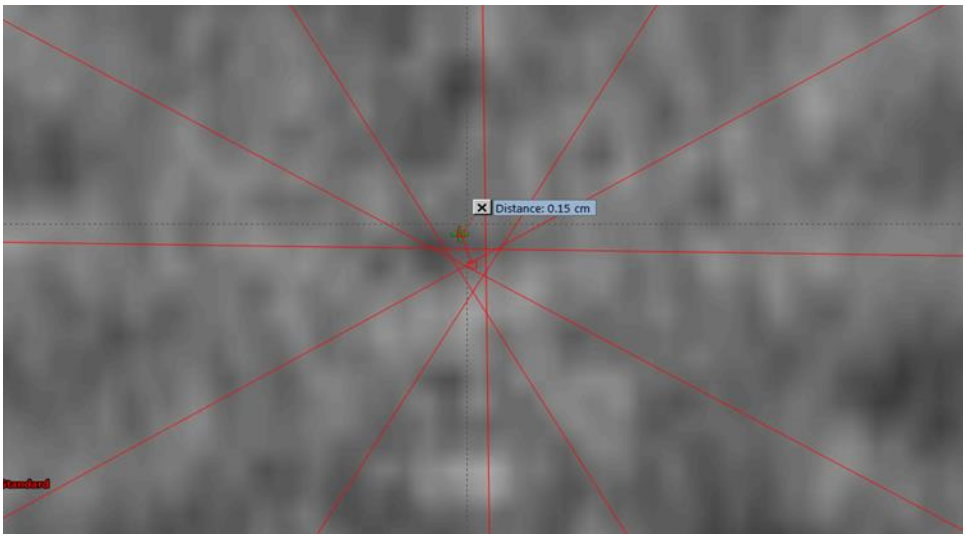

Figure 16: Collimator rotation star shot. (Extended zoomed isocentric scan)

Table 6: Radius of the smallest circle and vector deviations in comparison with film measurement

Rotations	**Radius of the smallest circle /cm**	**Distance of the center of the radius of the smallest center to the imaging isocenter**			**Film star shot from annual QA**
		R/cm	**Y/cm**	**X/cm**	
Gantry	0.05	0.01	0.01	0	0.048
Couch	0.03	0.13	0.13	0	0.029
Collimator	0.06	0.15	0.09	0.12	0.08

Note: R/cm is the total vector displacement with Y and X being the individual components of the vector

3. Film Dosimetry

Film is the gold standard for comprehensive dose verification in radiation oncology and is commonly used for verification of selected planes of spatially complex radiotherapy dose distributions. Radiochromic film provides 2D dose distribution information with a high spatial resolution. It consists of microcrystals which are based on radiation sensitive dye and embedded in a gelatin binder. Upon irradiation, a solid – state polymerization takes place and the film adopts a progressively blue color, which can be read out using a flatbed scanner to quantify quantification optical density. Since the radiochromic films are sensitive to ultraviolet light, fluorescent light, and to sunlight, they are read and handled in normal incandescent light.

According to Devic et al. (2005), Gafchromic film is designed to overcome the limitation of radiochromic film for external beam therapy. It is very promising for high – quality dosimetry in IMRT applications due to these features: improved sensitivity, improved post irradiation coloration, room temperature preparation and excellent image resolution (Coursey et al., 1998). Gafchromic EBT film, has an effective atomic number of 6.98 which makes it water equivalent (van Battum, Hoffmans, Piersma, & Heukelom, 2008). The film could be handled in existing interior light condition which is capable of producing reliable and reproducible dose measurements, with a high degree of spatial accuracy and uniformity of response (Aland, Kairn, & Kenny, 2011; van Battum et al., 2008) with no developer required (van Battum et al., 2008). The dose

response of the radiochromic film is typically measured by a flat- bed optical scanner. Since the absorption spectrum of radiochromic film exhibits a maximum in the red colour region of the visible spectrum, extraction of red colour channel information from a Red- Green- Blue (RGB) image represents the most frequently used procedure when using a document color scanner for the film dosimetry. Warm up effects, if present for the scanner in use, need to be investigated and considered in the dosimetry protocol. After scanning radiochromic films with document scanners, images can be saved in standard file formats, such as TIFF (Tagged Image File Format). Such files can then be imported into standard commercial software for film dosimetry or further processed in other research software platforms, e.g. MATLAB (The MathWorks, Inc., Natick, MA, USA) and fiji/image J. Using such software tools, dosimetric comparisons of line dose values (profiles) or gamma evaluation can be performed (Alber et al., 2008.).

3.1 Polymer Gel sheet Dosimetry

The purpose of this chapter is to apply the NIPAM-based dosimeter material as a thin (0.5-1cm) flat sheet with dual modality readout, thus combining the advantages of NIPAM-based dosimeters with those of film dosimetry. Our purpose is to enable read out of the dosimeter like traditional film using the optical flatbed scanner, as well as using kV-CBCT. CBCT has the advantage of automatically incorporating delivered dose into the imaging coordinate system, while flatbed scanner has the potential advantage of high precision dosimetry and being an already widely used technology for dosimetry

measurements. In addition to these advantages, the polymer gel dosimeter in a flat sheet could potentially serve as a bolus and a dosimeter combination. Also film dosimetry can be applied in many geometries by placing it within any phantom geometry.

3.2 Materials and methods

The laboratory production procedure of the flat gel dosimeter is the same with the CBCT-D except that in this case, the produced NIPAM gel is poured in a cellophane bag immediately after production so as to solidify in a flat position. It is then vacuum sealed and placed in a refrigerator sandwiched between two solid flat plates with weights placed on top so that the final shape of the dosimeter was a flat sheet. The thickness was then measured with a micrometer screw gauge after solidification. Forty-eight hours later, the flat gel was imaged (optical density and CT) and irradiated.

3.2.1 Flat-bed optical scanner

The EPSON (Expression 11000XL) flat -bed scanner located at Dosimetry unit of Duke Clinic was used for optical density scans. This scanner scans films in the transparent mode with a color depth up to 48 bits in the red – green - blue (RGB). White fluorescent xenon lamp is the light source in the transparency unit, which is located behind a diffuser. A charge –coupled device (CCD) splits the incident light spectrum into three measurable wavelength bands corresponding to the subtractive primary colors red, green, and blue. For traditional film measurements, film position is crucial to correct for polarization effects. Film calibration and dosimetry is performed with the

same film orientation (landscape or portrait) in the scanner of the film reading device (Alber et al., 2008).

Then optical density which is the degree to which the irradiated spots absorb transmitted rays of light is deduced using

Optical density = $\log_{10} I_0/I$

Where I is the transmitted intensity I_0 is the intensity of the un-irradiated region

Figure 17: EPSON flatbed scanner at Duke

Image/Fiji software (Schindelin et al., 2012) which opens Dicom files is used to analyze the optical density scan

3.2.2 Diagnostic CT scan

Given that this is the first evaluation of a polymer gel flat sheet; we performed our initial tests using a diagnostic CT, with the intent that these results will be applicable to future work using an on-board CBCT system. The flat gel is attached to solid water to

develop a buildup region for irradiation; and it also scanned in this position using the Diagnostic CT with the settings in Table 7**.**

Table 7: Diagnostic CT settings used in the scans

Scan options	Helical mode
Data collection Diameter	500mm
Reconstruction Diameter	493.0
Source detector Distance	1062.6mm
Source Patient Distance	605.9
Rotation Direction	Clockwise
X- ray tube current	750mA
X – ray tube voltage	120.0KV
Generator power	90000kw
Exposure	50mAs
Exposure time	1.281s
Focal spot	1.2mm
Filter type	Body filter
Convolution Kernel	Standard

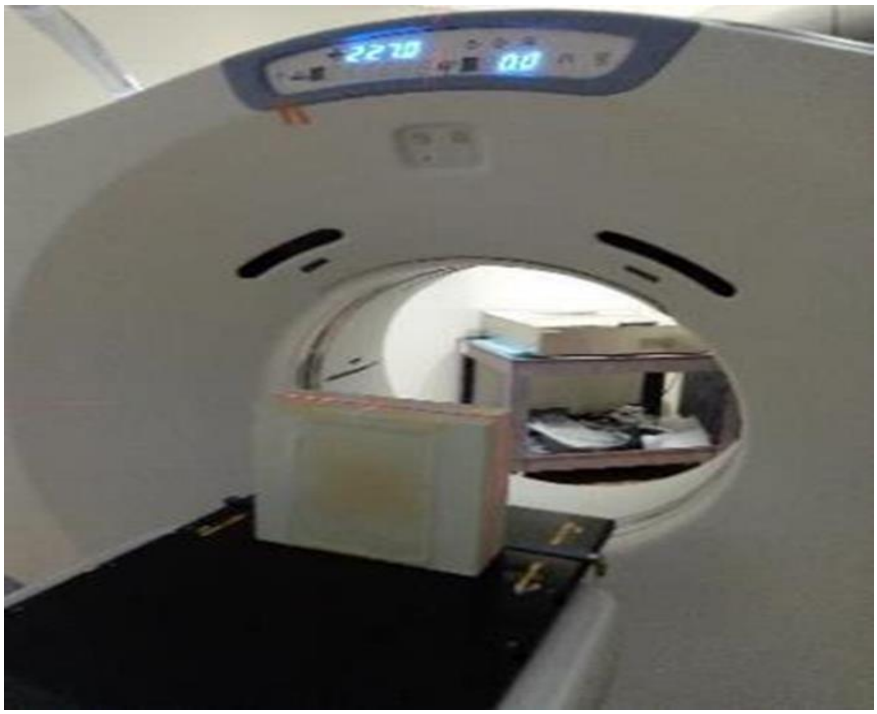

Figure 18: Flat gel attached to solid water and scanned with diagnostic CT

3.3 Irradiation

Irradiation was done at the Varian 600C/D linear accelerator which also uses 6MV photons similar to the TrueBeam STX but without the capability of CBCT imaging. For irradiation, a field size of 3 X 3cm and 100cm SSD is used. The following Monitor Units (MU's): 0, 25, 50, 75, 100, 200, 500, 1000, 1500 and 2000 MU's were used at different locations on the flat sheet dosimeter..

3.4 Results and Discussion

The produced flat gel weighs 0.365kg with a thickness of 5.71mm. An oxygen absorbers was used in making the flat shaped gel before vacuum sealing, however it was found that this caused significant artifacts on the resulting diagnostic images. For this reason, after irradiation but before performing a diagnostic CT, the portion of the dosimeter with the oxygen absorber was cut out.

3.4.1 Optical flatbed scanner & Diagnostic CT

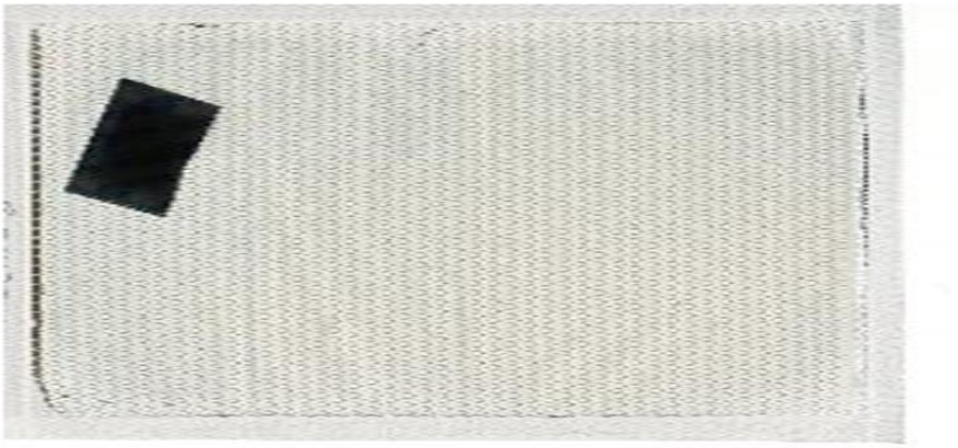

Figure 19: Pre-irradiated flat gel scan using the optical flat- bed scanner

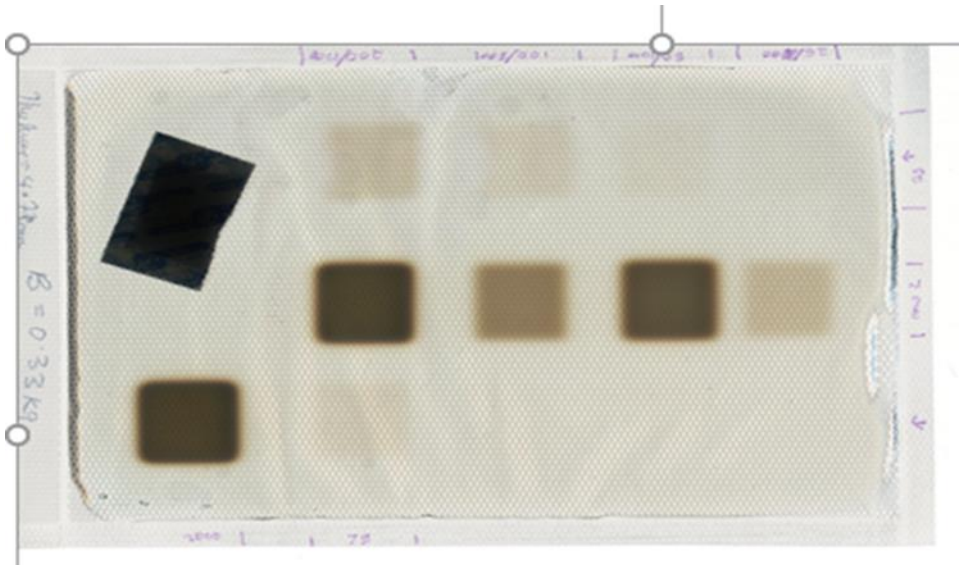

Figure 20: Post Irradiated flat gel scan using the optical flat- bed scanner

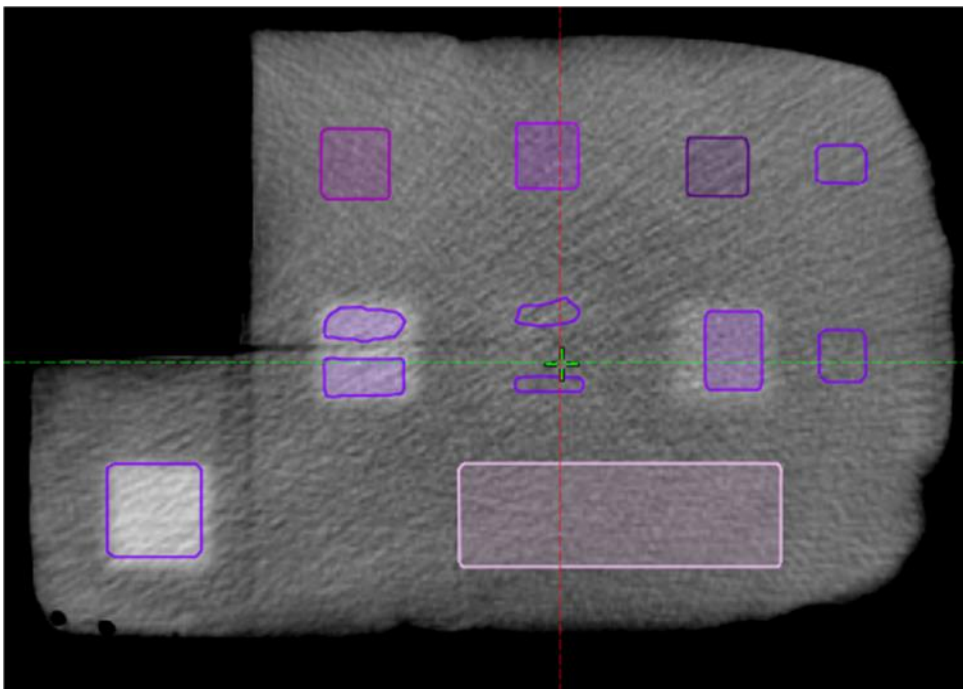

Figure 21: Diagnostic CT scan displaying how to take care of artefacts by preventing the dark spot in the mean CT numbers.

Note: The dark spot (the only spot in the pre-irradiated scan) is due to an oxygen absorber placed inside this dosimeter plane which was cut out (detached region in Figure 21) to avoid causing artefacts during scanning.

Both scans showed the increase in polymerization with dose in the irradiated fields with the optical scan displaying the spots with the degree of darkening; and the diagnostic scan displaying the spots with the degree of whitening. However, a number of artifacts were present in the CT image, which are characteristic of CT imaging.

3.4.1.1 Optical density

Table 8: Optical Density in all the color bands

This table shows the result of all the monitor units with its respective optical density for the RGB color channels. The optical density values increase with increasing monitor units in all the color channels. This is expected because the mass density change of NIPAM polymer gel following irradiation is proportional to the dose and could be used for calibration purposes. In each of the monitor units the red color channel had the least intensity value due to high wavelength of the light in this region. The blue channel showed the largest change in optical density with dose, and thus may be the best candidate for reading out the dose.

Monitor Units	*Optical Density*		
	Blue	**Green**	**Red**
0	0	0	0
25	0.030	0.022	0.026
50	0.043	0.030	0.028
75	0.056	0.033	0.024
100	0.066	0.044	0.038
200	0.110	0.075	0.060
500	0.346	0.255	0.192
1000	0.539	0.432	0.383
1500	0.648	0.512	0.461
2000	0.673	0.534	0.474

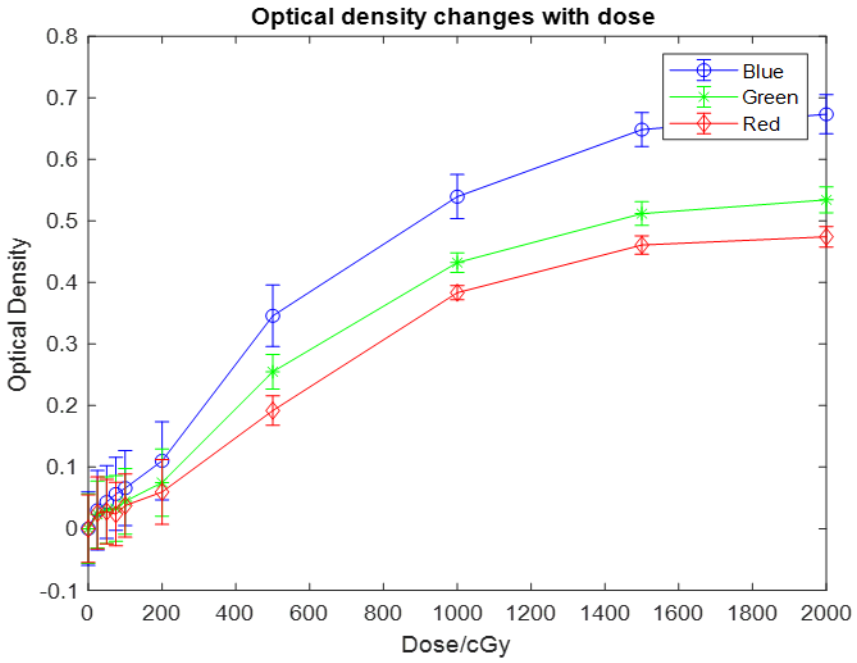

Figure 22: Graph of optical density changes with dose

All the irradiated spots displayed optical density values proportional to the radiation dose which supports feasibility of using the NIPAM polymer gel for dose measurement in all the color bands. The blue channel region gave the highest optical density read out with a wider margin (24%) when compared with the other two channels. Figure 23, Figure 24, Figure 25 and Figure 26 show the intensity profile across the dosimeter. The ribbed surface of the plastic bag causes the pattern in optical density.

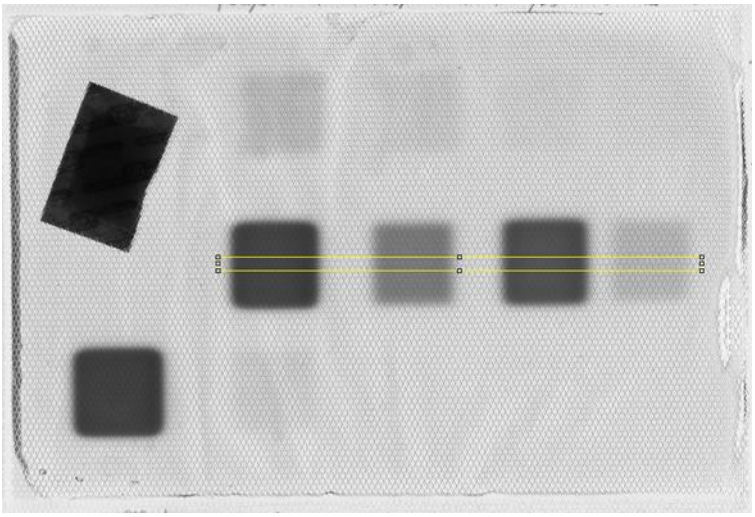

Figure 23: Location of intensity profile across flat sheet dosimeter.

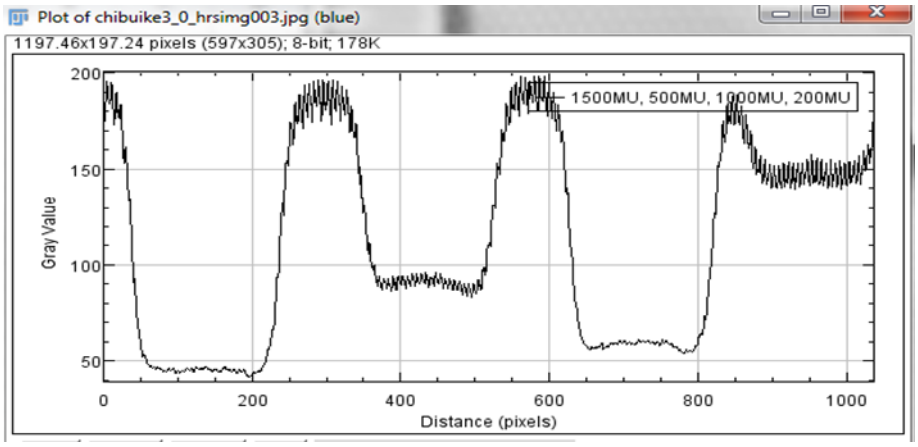

Figure 24: Intensity profile across flat sheet dosimeter for the blue color band

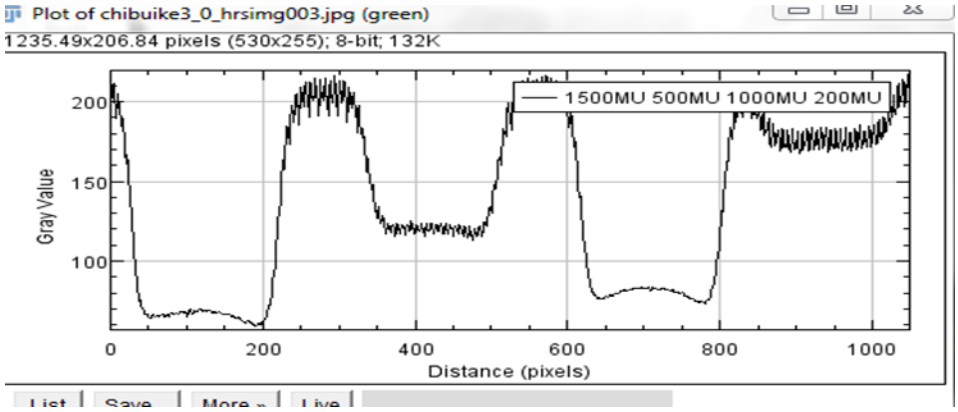

Figure 25: Intensity profile across flat sheet dosimeter for the Green color band

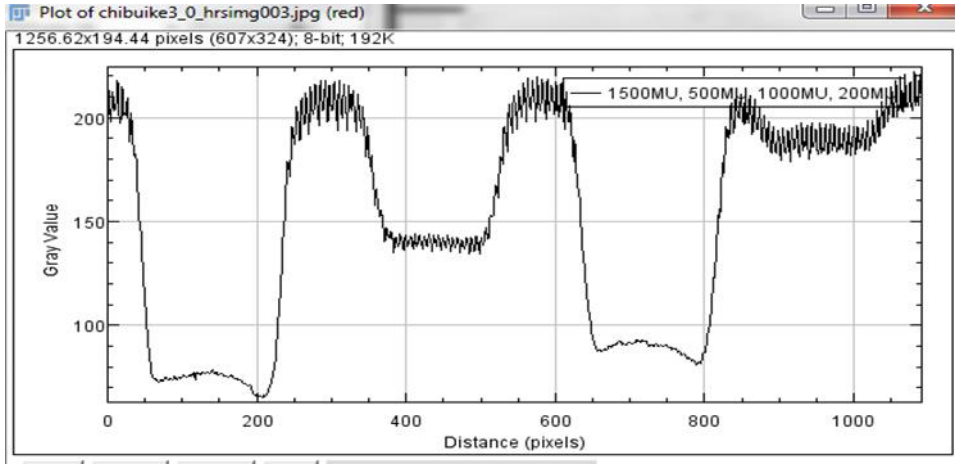

Figure 26: Intensity profile across flat sheet dosimeter for the Red color band

3.4.2 Dose intensity in kV-CT

In addition to reading dose with the flatbed scanner, a diagnostic CT was acquired of the flat sheet dosimeter and intensity quantified as a function of delivered Monitor Units. When possible, areas with obvious artifacts were excluded from the analysis when calculating mean CT intensity per irradiated area.

Table 9: Mean CT values and Standard deviation for the Monitor units

Monitor Units (MU)	*Mean CT*	*Standard deviation*
0	11.11	2.39
25	15.04	2.26
50	14.45	2.51
75	12.65	2.62
100	16.12	2.95
200	12.76	1.87
500	20.38	5.04
1000	21.11	3.06
1500	30.54	5.93
2000	29.37	4.77

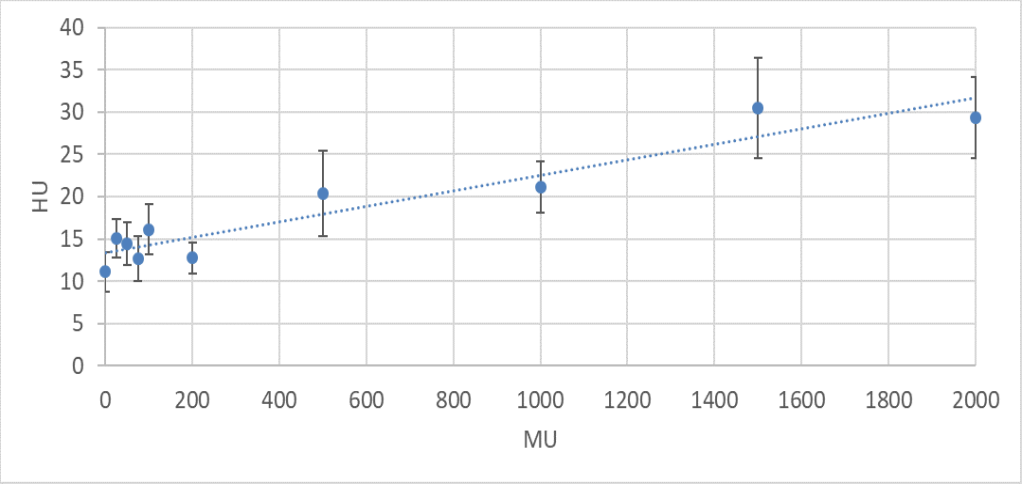

Figure 27: Graph of CT number with dose

At lower MU (0 – 200); the CT number tend to fluctuate which is probably due to background noise and dose scatter which affected the scanned polymerized spots. The contrast for the ROIs areas was not distinguishable from the background noise for these fields receiving 0-200MU. Above 200MU Figure 27 showed an increase in polymerization. The non-uniform uncertainty values from the trend line is also due to artefact, slice selection, and low sensitivity relative to the noise.

4. Conclusion

A spot check of the CBCT star shots showed that all spokes were easily visible which shows its potential for convenient isocenter QA for medical linear accelerators. Further analysis using the eclipse on the radius of the smallest circle showed that all the rotations were within the recommended tolerance limits specified by TG 142 (Klein et al., 2014). When compared with radiochromic film measurements, the Gantry and couch rotation showed <0.1mm difference, while the Collimator showed 0.2mm difference. This rotation showed no zero (0) value in all dimensions which is expected. The reason for the non –zero isocentricity is due to the mechanical imperfections of the rotating components of the linear accelerator, including sag from gravity. The gantry and couch rotations showed perfect alignment in R and X sides but a slight vertical displacement which is also expected due to the mechanical stability of their rotations.

The irradiated spots in the sheet were able to lead to varying degree of polymerization which depended in the MU value. We were able to generate the optical density values of each of the spots which symbolizes the degree of mass density change attenuating the light intensity during the optical scan for all the color bands. Subsequently, when fabricated in a smooth and very transparent bag, it could be used to determine the optical transmissivity, useable and best densities of the polymer gel when used as film. In addition, the calibration potential of the polymer sheet for both the

optical and diagnostic CT scan has now been established. This will be beneficial in dose measurement using the techniques of the traditional film.

One limitation of the sheet experiment was the presence of artefacts and the reconstruction ring artefact of CT scanner in the CT image. While no artifacts were visible in the 2000MU and 1000MU ROIs, artifacts were clearly present for the 1500MU and the 500MU ROIs. The 1500MU showed a dark line traversing the field; while the 500MU showed a dark area at the center which is also the center of the film. To combat this, the chosen ROIs for analysis should avoid areas that were clearly affected by artefacts. It is clear from Figure 27 that this measurement was also highly limited by noise in general. In future work this may be partially decreased by increasing the mAs or averaging. Another issue was partial volume averaging, due to the dosimeter was not perfectly aligned with the CT scanner, and variations in the dosimeter thickness. These issues will also need to be addressed in future work.

Appendix A

The steps using image/Fiji software for analysis

Step one: Split the Pre irradiated and post irradiated scanned images into several color components (Image-color-channels)

Step two: For each MU and color, get the mean, standard deviation, area, max and minimum values (Analyze-set measurement). Then crop it with a square selection. Press control T

Step three: For the answer you get in step three, press M to take all the selected measurements

Step four: copy to excel and deduce the optical density. (Equation 3.1); and plot the graph

Step five: Get the dose calibration for each of the color bands by cropping selected section of the image and press K

Appendix B

Manufacture of the NIPAM Polymer gel: The formulation process has 4 steps: Each step of the procedure is carefully controlled based on timing and temperature, to ensure reproducibility (1): Gelatin (300 Bloom Type A) was allowed to swell in the 75.5% of the de-ionized water for 10 min at room temperature, before heating to 45 ◦C. (2): While stirring continuously, Bis was dissolved at 45 °C, which took about 15 min, followed by addition of monomer (NIPAM). The gelatin–crosslinker mixture had to cool to approximately 37 °C. (3): A solution of the antioxidant THPC was added to the solution. The resulting gels were clear (the Bis gel was very faint yellow) and transparent. (4): The gel solutions were transferred into a plastic container with low oxygen permeability, and then closed with a sealing film. It took 25 minutes to heat the Gelatin to 45^0C. During this process, Bis and NIPAM were being prepared for addition by making exact measurement and manually squeezing some of the coagulated samples in the NIPAM which has been under refrigeration. Cooling of the gelatin – crosslinker to approximately 37^oC took about 30 minutes; no thanks to the inherent heating of the heating machine after being switched off.

The total production time is approximately 1 hour 20 minutes. Irradiation was done within 48 to 72 hours later depending on the availability of the Linac machine and the scanning was done immediately following irradiation. The total time from the start of production to scanning of the irradiated gels took between 49 hours 20 minutes to 73

hours 20 minutes. This timing duration is similar for both Cylindrical and flat shaped gel fabrication. Pouring the viscous gel into the cylindrical containers and vacuum sealing were quite simple; but the flat shaped gel required more attention in ensuring uniform thickness during refrigeration. In this case, we stretched the gel before vacuum sealing and then placed the flat shaped gel in between weight of materials (thick back text books) and placed inside the refrigerator. The shape of the gels were designed for verification of dosimetry potential. The cylindrical shaped gel was based on star shot feasibility while the flat shaped gel was based on spatial accuracy and calibration. Adaptation into various phantom shapes is very feasible and variation in noise, contrast and CNR is expected.

Precautions taken in the entire fabricating process were categorized for personnel safety and reduction of oxygen interference. The safety data sheet from the vendor (SIGMA - ALDRICH) has it that THPC is a category 1 hazard level for skin sensitization and serious eye damage, a category 4 level for oral ingestion and causes inhalation toxicity. So keen efforts were directed in ensuring safety using the chemical. We took advantage of the quarterly laboratory safety training organized by Duke Occupational and Environmental Safety Office which resulted in the development of the Standard Operating Procedure (SOP) for the use of THPC (Appendix C). For oxygen interference reduction, oil was used to displace the air above the surface of the gel before

closing the cylindrical container with light cellophane. It was then placed in a cellophane bag and vacuum sealed before refrigeration.

Appendix C

Standard Operating Procedure (SOP) for working with Tetrakis(hydroxymethyl)phosphonium chloride <THPC> (CAS: 124-64-1)

PI: Dr Justus Adamson

PI Signature:

Date: 08/13/2018

OESO Approval? Yes No

Departmental Approval? Yes No

Building(s): Davidson Bldg

Designated work Area: Fume Hood in 0003

OESO Signature:

Departmental Signature:

Hazard Identification

a. **Preparation and Use:**

- THPC shall be stored underneath chemical fume hood in flammables storage when not in use
- BEFORE taking THPC bottle out of the hood, make sure to equip eye protection (goggles or glasses), gloves and lab coat
- Quickly transfer the bottle into the fume hood

- With the fume hood slightly ajar, only enough for hands to pass through, use a pipette to draw out the chemical
- COMPLETELY SEAL the bottle before transferring the chemical back into the fume hood.

b. Potential Hazards and Risk:

- Toxic if swallowed or in contact with skin (H301-3, H311-3)
- Causes skin irritation (H315-2)
- Causes serious eye damage (H318-1)
- May cause allergy of asthma symptoms or breathing difficulties if inhaled (H3341)
- Toxic to aquatic life with long lasting effect (H401-2, H411-2)

Precautionary statements: Avoid breathing mist/vapors. Please check the attached SDS. Hazards: H301-H311-H315-H318-H334-H411. Precautions: P261-P273-P280-P301 + P310-P305 + P351 + P338-P342 + P311

Hazard Control

a. Selection and Purchasing:

- Sigma Aldrich 404861 – 500ml: If possible, purchase in small quantities or dilute solutions to minimize waste and reduce the risk of exposure

b. Engineering Controls:

- The experiment should be performed in a chemical fume hood. Eyewash station should be available in the event of an exposure

c. Administrative and Work Practice Controls:

- Read the attached Safety Data Sheet
- Plan work to avoid glove contact with chemical. Change gloves immediately if contaminated and at least every hour. Wash hands at time of glove change
- Consult Toxic & Health Hazard Liquid chemical safety guidelines before use; follow all precautions.

d. Personal Protective Equipment (PPE):

- Eyewear (safety glasses/goggles), gloves, lab coat

Storage and Transportation:

- To be stored at all times in nonflammable storage unit, completely sealed in a bottle, and away from strong oxidizing agents and bases.
- Keep container tightly closed in a dry and well – ventilated place. Containers which are opened must be carefully resealed and kept upright to prevent leakage.
- Transport toxic liquids in secondary containment, preferably a polyethylene or other non-reactive acid/solvent bottle carrier.

Emergencies, Spill Procedures, and Exposures/Unintended Contact

Emergencies:

- If on skin or hair, remove contaminated clothing and PPE and rinse area in sink or safety shower for a minimum of 15 minutes.
- If in eyes, remove glasses or googles and rinse eye at eye wash station for a minimum of 15 minutes.
- If inhaled, move to a location with fresh air and rest in a position comfortable for breathing.
- In the event of any exposure, fill out the work-related injury or illness report found at: https://www.hr.duke.edu/forms/workcomp/.
- Depending upon your employment status (minor, undergraduate student, employee, etc.), additional steps may be required. Ensure you know your individual response procedure for injuries.

If needed, Contact Employee Occupational Health and Wellness (EOHW) at 919-684-3136 for medical advice on occupational chemical exposure.

Chemical Spills:

If spill is less than 500 mL in a fume hood, use spill kit located underneath lab sink to clean-up spill. Wearing appropriate gloves, splash goggles, lab coat, use an inert absorbent material (vermiculite, dry sand) to clean up the spill. Contaminated PPE and

clean-up materials must be placed in a sealed container for pick-up by OESO (see waste disposal section for more information).

If spill is greater than 500 mL in a fume hood or any size outside a fume hood, call OESO spill response team at 911 from a campus phone or 919-684-244 (Duke Police) from any phone.

Notes: On the Durham campus, "large" spills of volatile or powdered hazardous materials and all mercury spills must be referred to the OESO spill response team by calling **911** from a campus phone or **919-684-2444** from any phone. Contact Employee Occupational Health and Wellness (EOHW) at 919-684-3136 for medical advice on occupational chemical exposures. For an actual chemical exposure, complete the work-related injury or illness report found at: https://www.hr.duke.edu/forms/workcomp/.

Waste

- Store waste in sealed bottle if needed and minimize waste THPC where possible.
- Do not flush to sanitary sewer or waterway.
- Handle and store hazardous wastes following the guidelines above while accumulating wastes and awaiting chemical waste pickup.
- Toxic wastes must be disposed of following Duke University's Chemical Waste Policy and the Laboratory Chemical Waste Management Practices.

These policies cover container management and procedures and timelines for chemical waste pickup.

Details of Process

Follow the gel production process and know when to use the THPC

Training

All personnel are required to complete the online General Lab Safety session though the OESO website. This session includes an introduction to general chemical safety. Furthermore, all personnel shall read and fully adhere to this SOP when handling the chemical.

Appendix D

Dosimeter imaging procedure and parameters: CBCT-D: The gel is first immobilized with tape to the couch to prevent motion during the QA procedure.

Figure 28: CBCT-D set up of the gel for all-star shots

Imaging is done using the CBCT optimized setting before and after the gel irradiation. The optimal values we decided for our CBCT setting were full trajectory, smooth reconstruction filter, strong ring suppression and 80KV. At this point, there was an upgrade so that the Ring Suppression could no longer be modified easily, so it was kept constant at the clinical setting (Medium) for later CBCT acquisitions. Other

parameters include full fan type, CTDIw: 10.74cGy, Matrix size: 512, and Slice thickness: 2mm.

Sheet Dosimetry: Imaging was done using The EPSON (Expression 11000XL) flat -bed scanner and Diagnostic CT all located at the Radiation Oncology Department of Duke Clinic. For each case, pre and post irradiation scans were made. For the optical scan, the orientation of the sheet film is placed in the portrait position like the traditional film. The position of the film in noted and maintained for both scans. For the Diagnostic CT imaging, The flat gel is attached to solid water to develop a buildup region for irradiation; and it also scanned in this position using the Diagnostic CT with the settings in Table 10**.**

Table 10: Diagnostic CT settings used in the scan

Scan options	Helical mode
Data collection Diameter	500mm
Reconstruction Diameter	493.0
Source Detector Distance	1062.6mm
Source Patient Distance	605.9
Rotation Direction	Clockwise
X – ray tube current	750mA
X – ray tube voltabe	120.0KV

Generating power	90000Kw
Exposure time	1.281s
Focal spot	1.2mm
Filter type	Body filter
Convolution kernel	Standard

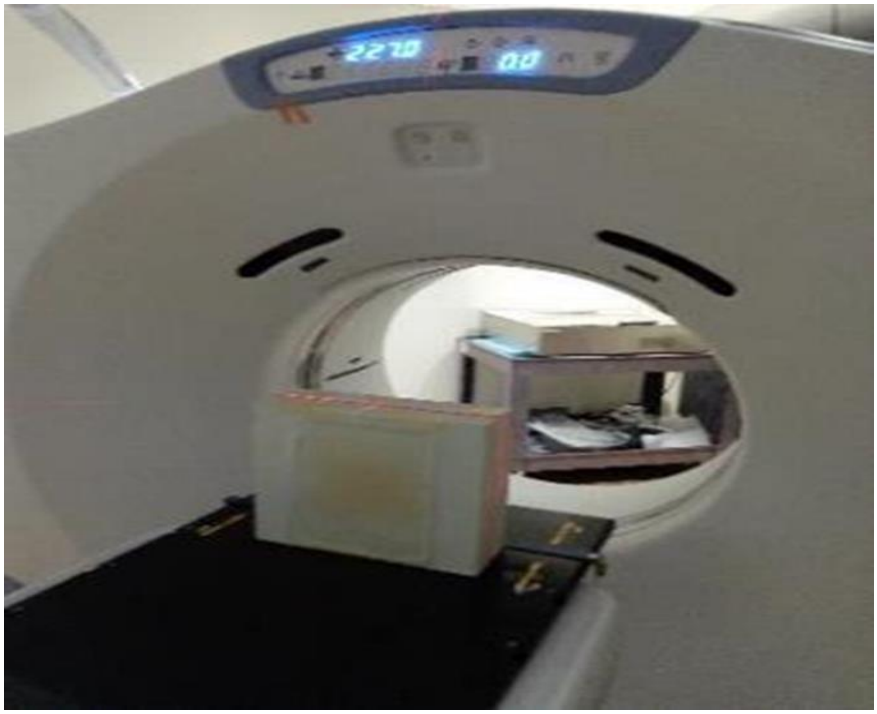

Figure 29: Flat gel attached to solid water and scanned with diagnostic CT

The change in linear attenuation coefficient (μ) due to irradiation is a result of the change in electron density caused by the displacement of water in the polymerized spots. This is determined by the change in CT number (N_{CT}). $N_{CT} = 1000 \times (\mu - \mu_w)/ \mu_w$ where μ_w is the linear attenuation coefficient of water. The change in density ($\Delta\varrho$)

becomes directly proportional to the change in CT number (ΔN_{CT}). $\Delta\rho = k\Delta N_{CT}$ where k is a constant (function of the unirradiated gel).

Heat load effect on the Anode: This was studied for different KV and mAs with the goal of considering the effect of anode heat on our KV selection.

Table 11: Average increase in heat unit(ΔU) for different KV

KV	***ΔU***	***mAs***	***ΔU/mAs***
40	5.3	640	0.0083
60	8.3	640	0.0130
80	10	640	0.0156
120	4	160	0.0250
140	4.3	160	0.0269

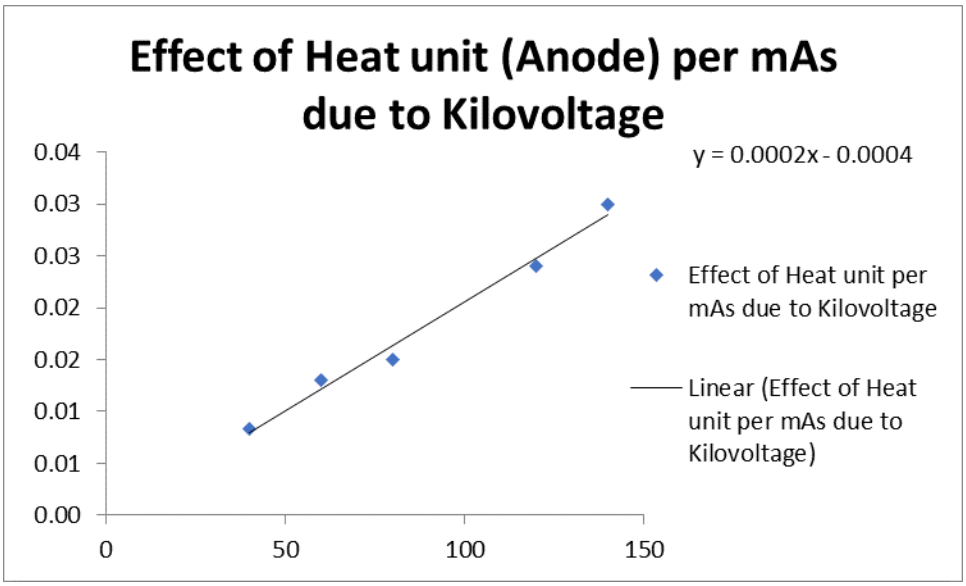

Figure 30: Graph of Heat unit per mAs due to Kilovoltage

Slope: 0.0021 and Intercept: -0.00043

Table 12: Selected KVs and their effect on anode heat load per mAs.

KV	*ΔU/mAs*
125	0.026
100	0.021
80	0.016

The 80KV showed the least heat effect on the anode per mAs as seen in Table 12

Bibliography

Adamson, J., Carroll, J., Trager, M., Yoon, S. W., Kodra, J., Maynard, E., … Jirasek, A. (2018). Delivered dose distribution visualized directly with on-board kV-CBCT: proof of principle. *International Journal of Radiation Oncology*Biology*Physics*. https://doi.org/10.1016/J.IJROBP.2018.12.023

Aland, T., Kairn, T., & Kenny, J. (2011). Evaluation of a Gafchromic EBT2 film dosimetry system for radiotherapy quality assurance. *Australasian Physical & Engineering Sciences in Medicine*, *34*(2), 251–260. https://doi.org/10.1007/s13246-011-0072-6

Alber, M., Broggi, S., De Wagter, C., Eichwurzel, I., Engström, P., Fiorino, C., … Welleweerd, H. (2008). *GUIDELINES FOR THE VERIFICATION OF IMRT*. Retrieved from https://www.estro.org/binaries/content/assets/estro/school/publications/booklet-9---guidelines-for-the-verification-of-imrt.pdf

Baldock, C., De Deene, Y., Doran, S., Ibbott, G., Jirasek, A., Lepage, M., … Schreiner, L. J. (2010). Polymer gel dosimetry. *Physics in Medicine and Biology*, *55*(5), R1-63. https://doi.org/10.1088/0031-9155/55/5/R01

Bedford, J. L., Lee, Y. K., Wai, P., South, C. P., & Warrington, A. P. (2009). Evaluation of the Delta ^{4} phantom for IMRT and VMAT verification. *Physics in Medicine and Biology*, *54*(9), N167–N176. https://doi.org/10.1088/0031-9155/54/9/N04

Brindha, S., Venning, A. J., Hill, B., & Baldock, C. (2004). Experimental study of attenuation properties of normoxic polymer gel dosimeters. *Physics in Medicine and Biology*, *49*(20), N353–N361. https://doi.org/10.1088/0031-9155/49/20/N01

Catphan 500 — The Phantom Laboratory. (n.d.). Retrieved February 11, 2019, from https://www.phantomlab.com/catphan-500

Coursey, B. M., Gall, K. P., Galvin, J. M., Mclaughlin, W. L., Meigooni, A. S., Nath, R., … Blackwell, C. R. (1998). *Radiochromic Film Dosimetry Radiochromic film dosimetry: Recommendations of AAPM Radiation Therapy Committee Task Group 55*. *MEDICAL PHYSICS* (Vol. 25). Retrieved from https://www.aapm.org/pubs/reports/rpt_63.pdf

De Deene, Y., De Wagter, C., Van Duyse, B., Derycke, S., De Neve, W., & Achten, E. (1998). Three-dimensional dosimetry using polymer gel and magnetic resonance imaging applied to the verification of conformal radiation therapy in head-and-neck cancer. *Radiotherapy and Oncology*, *48*(3), 283–291. https://doi.org/10.1016/S0167-8140(98)00087-5

Deene, Y. De, Venning, A., Hurley, C., Healy, B. J., & Baldock, C. (2002). Dose$ndash$response stability and integrity of the dose distribution of various polymer gel dosimeters. *Physics in Medicine and Biology*, *47*(14), 307. https://doi.org/10.1088/0031-9155/47/14/307

Depuydt, T., Penne, R., Verellen, D., Hrbacek, J., Lang, S., Leysen, K., … Ridder, M. De. (2012). Computer-aided analysis of star shot films for high-accuracy radiation therapy treatment units. *Physics in Medicine and Biology*, *57*(10), 2997–3011. https://doi.org/10.1088/0031-9155/57/10/2997

Devic, S., Seuntjens, J., Sham, E., Podgorsak, E. B., Schmidtlein, C. R., Kirov, A. S., & Soares, C. G. (2005). Precise radiochromic film dosimetry using a flat-bed document scanner. *Medical Physics*, *32*(7Part1), 2245–2253. https://doi.org/10.1118/1.1929253

Fong, P. M., Keil, D. C., Does, M. D., & Gore, J. C. (2001). Polymer gels for magnetic resonance imaging of radiation dose distributions at normal room atmosphere. *Physics in Medicine and Biology*, *46*(12), 3105–3113. https://doi.org/10.1088/0031-9155/46/12/303

González, S. ., Bonomi, M. ., Santa Cruz, G. ., Blaumann, H. ., Larrieu, O. A. C., Menéndez, P., … Roth, B. M. . (2004). First BNCT treatment of a skin melanoma in Argentina: dosimetric analysis and clinical outcome. *Applied Radiation and Isotopes*, *61*(5), 1101–1105. https://doi.org/10.1016/J.APRADISO.2004.05.060

Gustavsson, H., Karlsson, A., Bäck, S. Å. J., Olsson, L. E., Haraldsson, P., Engström, P., & Nyström, H. (2003). MAGIC-type polymer gel for three-dimensional dosimetry: Intensity-modulated radiation therapy verification. *Medical Physics*, *30*(6), 1264–1271. https://doi.org/10.1118/1.1576392

Hilts, M., Audet, C., Duzenli, C., & Jirasek, A. (2000). Polymer gel dosimetry using x-ray computed tomography: a feasibility study. *Physics in Medicine and Biology*, *45*(9), 2559–2571. Retrieved from http://www.ncbi.nlm.nih.gov/pubmed/11008956

Hilts, M., Jirasek, A., & Duzenli, C. (2005). Technical considerations for implementation of x-ray CT polymer gel dosimetry. *Physics in Medicine and Biology*, *50*(8), 1727–1745. https://doi.org/10.1088/0031-9155/50/8/008

Jirasek, A., Carrick, J., Hilts, M., Jirasek, A., Carrick, J., & Hilts, M. (2012). An x-ray CT polymer gel dosimetry prototype: I. Remnant artefact removal. *Physics in Medicine and Biology*. https://doi.org/10.1088/0031-9155/57/10/3137

Jirasek, A., Hilts, M., & McAuley, K. B. (2010). Polymer gel dosimeters with enhanced sensitivity for use in x-ray CT polymer gel dosimetry. *Physics in Medicine and Biology*. https://doi.org/10.1088/0031-9155/55/18/002

Jirasek, A., Johnston, H., & Hilts, M. (2015). Dose rate properties of NIPAM-based x-ray CT polymer gel dosimeters. *Physics in Medicine and Biology*, *60*(11), 4399–4411. https://doi.org/10.1088/0031-9155/60/11/4399

Johnston, H., Hilts, M., & Jirasek, A. (2015). Incorporating multislice imaging into x-ray CT polymer gel dosimetry. *Medical Physics*. https://doi.org/10.1118/1.4914419

Klein, E. E., Hanley, J., Bayouth, J., Yin, F., Simon, W., Dresser, S., … Holmes, T. (2014). Task Group 142 report : Quality assurance of medical acceleratorsa) Task Group 142 report : Quality assurance of medical accelerators a …, *4197*(121). https://doi.org/10.1118/1.3190392

Mather, M. L., Whittaker, A. K., & Baldock, C. (2002). Ultrasound evaluation of polymer gel dosimeters. *Physics in Medicine and Biology*, *47*(9), 1449–1458. Retrieved from http://www.ncbi.nlm.nih.gov/pubmed/12043812

Maynard, E., Hilts, M., Heath, E., & Jirasek, A. (2017). Evaluation of accuracy and precision in polymer gel dosimetry: *Medical Physics*. https://doi.org/10.1002/mp.12080

Mcjury, M., Oldham, M., Cosgrove, V. P., Murphy, P. S., Doran, S., Leach, M. O., … Murphy, P. S. (2000). *Radiation dosimetry using polymer gels: methods and applications*. *The British Journal of Radiology* (Vol. 73). Retrieved from https://www.birpublications.org/doi/pdf/10.1259/bjr.73.873.11064643

Oldham, M., Siewerdsen, J. H., Shetty, A., & Jaffray, D. A. (2001). High resolution gel-dosimetry by optical-CT and MR scanning. *Medical Physics*, *28*(7), 1436–1445. https://doi.org/10.1118/1.1380430

Pak, F., Farajollahi, A., & Miabi, Z. (2012). SU-E-T-150: The Basic Dosimetric Properties of NIPAM Polymer Gel Dosimeter. *Medical Physics*, *39*(6Part12), 3737–3737. https://doi.org/10.1118/1.4735208

Pak, F., Farajollahi, A., Movafaghi, A., & Naseri, A. (2013). Influencing Factors on Reproducibility and Stability of MRI NIPAM Polymer Gel Dosimeter. *BioImpacts : BI*, *3*(4), 163–168. https://doi.org/10.5681/bi.2013.019

Petoukhova, A. L., van Egmond, J., Eenink, M. G. C., Wiggenraad, R. G. J., & van Santvoort, J. P. C. (2011). The ArcCHECK diode array for dosimetric verification of

HybridArc. *Physics in Medicine and Biology*, *56*(16), 5411–5428. https://doi.org/10.1088/0031-9155/56/16/021

Schindelin, J., Arganda-Carreras, I., Frise, E., Kaynig, V., Longair, M., Pietzsch, T., … Cardona, A. (2012). Fiji: an open-source platform for biological-image analysis. *Nature Methods*, *9*(7), 676–682. https://doi.org/10.1038/nmeth.2019

Senden, R. J., Jean, P. De, McAuley, K. B., & Schreiner, L. J. (2006). Polymer gel dosimeters with reduced toxicity: a preliminary investigation of the NMR and optical dose–response using different monomers. *Physics in Medicine and Biology*, *51*(14), 3301–3314. https://doi.org/10.1088/0031-9155/51/14/001

Tamponi, M., Bona, R., Poggiu, A., & Marini, P. (2015). A practical tool to evaluate dose distributions using radiochromic film in radiation oncology. *Physica Medica*, *31*(1), 31–36. https://doi.org/10.1016/J.EJMP.2014.07.009

Trapp, J. V, Bäck, S. Å. J., Lepage, M., Michael, G., & Baldock, C. (2001). An experimental study of the dose response of polymer gel dosimeters imaged with x-ray computed tomography. *Physics in Medicine and Biology*, *46*(11), 2939–2951. https://doi.org/10.1088/0031-9155/46/11/312

Trapp, J. V, Michael, G., Deene, Y. de, & Baldock, C. (2002). Attenuation of diagnostic energy photons by polymer gel dosimeters. *Physics in Medicine and Biology*, *47*(23), 4247–4258. https://doi.org/10.1088/0031-9155/47/23/310

van Battum, L. J., Hoffmans, D., Piersma, H., & Heukelom, S. (2008). Accurate dosimetry with GafChromic™ EBT film of a 6MV photon beam in water: What level is achievable? *Medical Physics*, *35*(2), 704–716. https://doi.org/10.1118/1.2828196